Helmholtz-Zentrum
hereon

Final Draft
of the original manuscript

Zhou, S.; Di Luca, M.; Xu, X.; Ma, N.; Jung, F.; Lendlein, A.:

Defeating antibiotic-resistant bacteria with protein-resistant polyGGE film.

In: Clinical Hemorheology and Microcirculation. Vol. 79 (2021) 4, 609 - 623.

First published online by IOS: 03.08.2021

https://dx.doi.org/10.3233/CH-211250

Defeating antibiotic-resistant bacteria with protein-resistant polyGGE film

Shuo Zhou[1, 2], Mariagrazia Di Luca[3], Xun Xu[1], Nan Ma[1, 4], Friedrich Jung[1], Andreas Lendlein[1, 2, 4, *]

[1]Institute of Active Polymers and Berlin-Brandenburg Centre for Regenerative Therapies, Helmholtz-Zentrum Hereon, 14513 Teltow, Germany

[2]Institute of Chemistry, University of Potsdam, 14476 Potsdam, Germany

[3]Berlin-Brandenburg Centre for Regenerative Therapies, 13353 Berlin, Germany

[4]Institute of Chemistry and Biochemistry, Freie Universität Berlin, 14195 Berlin, Germany

* To whom correspondence should be addressed:

Prof. Dr. Andreas Lendlein, Institute of Active Polymers, Helmholtz-Zentrum Hereon, Kantstr. 55, 14513 Teltow, Germany email: andreas.lendlein@hereon.de

Abstract

Biofouling on medical device surfaces, which is initiated by protein adsorption and adhesion of microbes especially the antibiotic-resistant bacteria, attracts global attention for centuries due to its enduring challenges in healthcare. Here, the antifouling effect of hydrophilic poly(glycerol glycidyl ether) (polyGGE) film is explored in comparison to hemocompatible and protein-resistant control polymers. The chemical and thermomechanical stability of polyGGE in hydrated conditions at body temperature was achieved via adjusting UV curing and KOH quenching time. The polyGGE surface is inert to the plasma protein adsorption and interfered the metabolism conditions, biofilm formation and growth of both Gram negative (Gram-) and antibiotic-resistant Gram positive (Gram+) bacteria. These results indicate the potential application of polyGGE for combating the risk of hospital-acquired infections and preventing drug-resistant superbug spreading.

Introduction

Biofouling, the contamination of surfaces by accumulation of microorganisms, which can lead to life-threatening infections, is initiated by protein adsorption and microbial adhesion. In the clinic, it has been reported occurring on biomaterial surfaces and medical devices such as catheters, contact lenses, surgical equipment and medical implants [1]. It has been a long-lasting challenge in terms of healthcare [2]. Approximately 80% bacterial infections involve biofouling and almost half of the hospital derived infection are contamination of medical device related [3]. Therefore, antifouling becomes a global priority.

Basically, three major steps including bacterial contact, attachment, and biofilm growth are involved in the biofouling on biomaterial surfaces [4,5]. Depending on the surface properties of a device such as chemical structure, topography, hydrophobicity, surface charge and rigidity, the initial bacterial close contact is mediated by a variety of extracellular organelles and proteins for mechanosensing including flagella, pili, fimbriae, curli fibers and outer membrane proteins. The substrates where bacteria attached are immersed in fluids containing electrolytes and macromolecules. These soluble components adsorb on and can further alter the intrinsic physicochemical properties of the original surfaces. Second, bacteria irreversibly attach to the surfaces within several hours, which is mainly facilitated by the production of extracellular polymeric substance (EPS). Last, adherent bacteria start to replicate and form colonies to promote biofilm growth. These bacteria continuously secrete EPS and are encapsulated in a hydrogel, which provides a physical barrier between the bacteria community and the extracellular environment. The composition of EPS varies between species and growth conditions, and biochemical communication and physical contact between cells in the community stimulates its formation and secretion [6].

Prevention of biofouling mainly relies on the replacement of contaminated surfaces and antibiotic treatments, which are sometimes problematic due to the different architectures of bacterial cell envelopes. For instance, Gram+ bacteria usually possess a thick cell wall while Gram- bacteria with a thin cell wall harbor an additional outer membrane, which may conferring different responses of bacteria to external stresses including antibiotics [7]. A main factor causing the inefficacy of antibiotic administration is the persistence of antibiotic-resistant bacteria. Infection with antibiotic-resistant bacteria is difficult and in many cases impossible to treat. The relevant mechanism for this effect is mainly based on the remolding and reducing affinity of the cell wall composites, which are responsible for antibiotic binding

[8]. In addition, EPS may be involved in the development of antibiotic-resistant feature of bacteria [9].

There is a substantial demand to design and create an antifouling surface, which not only inhibits protein adsorption, bacterial adhesion and growth, but also can effectively eliminate antibiotic-resistant bacteria. Polyethylene glycol (PEG) is commonly used as a material for surface passivation to prevent non-specific protein binding and cellular uptake of drug or vaccine delivery vehicles [10]. PEG is also reported as one of the promising candidates for combating biofouling [11]. However, the linear PEG is hard to be further functionalized due to its limited reactive sites [12]. Degraded low molecular weight PEG is potentially toxic, and PEG displays a potential to cause immunogenicity [13]. Moreover, PEG used as a chemical additive for COVID-19 mRNA vaccine has recently shown to trigger anaphylaxis [14].

In the present study, poly(glycerol glycidyl ether) (polyGGE) was synthesized from glycerol glycidyl ether (GGE) monomers based on cationic ring opening polymerization [15]. Diphenyliodonium hexafluorophosphate (DPIHFP) was selected as a photoinitiator due to its high efficiency of superacid generation [16]. When GGE-DPIHFP mixture was irradiated by UV, photolysis occurred instantly to produce reactive radical cations and trigger hydrogen atom abstraction from GGE. Self-propagation of polymer chain was realized by continuous opening of epoxide. The reaction was terminated by exposure to an aqueous KOH solution, the ductility, chemical and thermomechanical stabilities of polyGGE in wet condition at physiological temperature were evaluated. The protein adsorption of major plasma proteins, bacterial metabolism, biofilm formation and growth of both *E. coli* and MRSA on polyGGE were investigated.

Materials and Methods

Synthesis of polyGGE film

Glycerol glycidyl ether (GGE, Raschig GmbH, Ludwigshafen am Rhein, Germany) was used as the monomer for the synthesis of polyGGE and DPIHFP (Sigma-Aldrich GmbH, Steinheim, Germany) as photoiniator. The reaction was based on a one-step cationic ring opening polymerization using monomer - photoinitiator mixture without any additional solvents as described in [15]. Photolysis of the initiator took place immediately after UV irradiation. Cleavage of Ph-I bonds yields reactive radical cations. Those radical cations were postulated to undergo hydrogen abstraction from GGE monomer to yield Brønsted acid and initiating the

polymerization. The crosslinker GGE itself could be used as the monomer to further make the crosslinking. The initial mixture was poured into a mould formed by two glass slides (10 cm × 10 cm), which has been pre-silanized. A Teflon frame with a thickness of 0.5 mm is placed in between as the spacer to determine the thickness of the final product. Photopolymerization is performed with SCU-110 mercury lamp (Uvexs, Sunnyvale, USA), which was placed with a distance of 5 cm to the glass slides. The mercury lamp emitted the UV peak at 365 nm wavelength, which was above that at which the silanized glass plates showed any significant absorbance. Cationic ring opening polymerization was terminated by adding 1 mol/L KOH aqueous solution for 24 h. For elasticity analysis in wet condition, thermostability analysis, protein resistance and antifouling tests, the crude polyGGE was extracted by ethanol in soxhlet for one week then dried at 60 °C in a high vacuum for one week until the weight reaches a constant value.

Tensile testing

Mechanical properties including Young's modulus and elongation at break of polyGGE with various UV exposure time in dry condition at room temperature were determined on a Zwick tensile tester (2.5N1S, Zwick GmbH & Co, Ulm, Germany) with a force transducer of maximum 50 N. Mechanical properties in wet conditions were determined on Zwick (ZP 99, Zwick GmbH, Ulm, Germany), equipped with a force transducer of maximum 20 N in a water chamber (distilled water), which was pre-heated to 37 °C. In both conditions, polyGGE samples were shaped to 30 mm × 2 mm according to ISO 527-2/1BB with thickness of 0.45 mm and elongated with a speed of 2 mm/min using a preforce of 15 mN. For the test in wet condition, samples were swollen for 24 h in distilled water to reach an equilibrium state.

Proton nuclear magnetic resonance spectroscopy (^{1}H NMR)

^{1}H-NMR spectra were recorded at 25 °C with a Bruker Avance 500 spectrometer (500 MHz, Bruker, Karlsruhe, Germany) with a relaxation time of 2 s. Dimethyl sulfoxide-D6 (Sigma-Aldrich GmbH, Steinheim, Germany) was used as an internal standard. To eliminate the unreacted epoxide, KOD solution (1 mol/L in D_2O) was used for quenching the polyGGE after UV curing for 30 min. Proton spectra were recorded after samples swollen in KOD solution for 0, 4, 24 and 72 h.

Water uptake ability

Dry weight of polyGGE films with different UV curing times was determined (W_d) prior to immersing samples in distilled water at room temperature. The swollen samples were taken out and the surfaces were gently blotted with filter paper to remove the unbound water. Weight of the swollen sample (W_{sw}) was measured after 1, 4, 20 and 24 h. The water uptake was calculated according to the formula: $\frac{W_{sw}-W_d}{W_d} \times 100\ \%$.

Wettability measurement

Water contact angle measurements were performed with a DSA 100 analyzer (Krüss GmbH, Hamburg, Germany) using the captive bubble method in a water–air system. Advancing and receding contact angles were measured by stepwise withdrawing/adding of air from/to the captured bubble, while the bubble was increased with each measurement cycle from 2 to 5 mm in diameter. Prior to the measurement, all samples were preconditioned for 24 h in deionized water at ambient temperature for equilibration. At least ten measurements on two different locations were performed on each sample and averaged to yield the mean values contact angles and their standard deviation.

Thermogravimetric analysis (TGA)

The thermal degradation of 30 min UV-cured, 24 h KOH quenched and one week 60 °C dried polyGGE was conducted on a TG209 instrument (Netzsch, Selb, Germany) at a constant heating rate of 10 °C/min between 25 and 600 °C under a nitrogen purge.

Differential scanning calorimetry (DSC)

DSC experiments were performed on DSC 204 Phoenix calorimeter (Netzsch, Selb, Germany) at heating of 10 °C/min in sealed aluminum pans. 30 min UV-cured, 24 h KOH quenched and one week 60 °C dried polyGGE were heated up from -70 °C to 200 °C before the cooling run to -70 °C at 10 °C/min, followed by the second heating run up to 200 °C at 10 °C/min. The glass transition temperature (T_g) was determined from the second heating run.

Control polymers for protein resistance and antifouling assays

Medical grade polytetrafluoroethylene (PTFE) and polydimethylsiloxane (PDMS) films were purchased from Bess Medizintechnik GmbH (Berlin, Germany).

Human platelet-poor plasma preparation

The study was designed and performed according to the current guidelines of the British committee for standards in hematology as well as of the International Society on Thrombosis and Haemostasis [17,18]. The study protocol was approved by the ethics committee of the Charite University Medicine Berlin (EA2-018-16). According to the criteria of the Nordkem-workshop [19], blood was taken from apparently healthy subjects, who received no platelet function inhibitors or other pharmaceuticals for at least 10 days [20]. Blood donation was carried out in the morning between 8:30 a.m. and 9:00 a.m. Blood was obtained from the cubital vein by an experienced phlebotomist using a standardized, atraumatic protocol, and was collected in S-Monovettes (Sarstedt AG & Co., Nümbrecht, Germany) filled with sodium citrate as anticoagulant (final concentration 0.106 mol/L; Sigma-Aldrich GmbH, Steinheim, Germany). During and immediately after blood collection, tubes were slowly agitated to ensure an appropriate mixing of anticoagulant and blood (and discarded if there was any evidence of clotting). Platelet-poor plasma (PPP) was obtained immediately by centrifugation of whole blood at 2000 x g for 20 min. The experiments were started 30 min after blood collection and were terminated 4 h later [21].

Plasma protein adsorption

300 µL of platelet-poor plasma was added onto the surface of the samples (with Teflon ring) in 48-well tissue culture plates, the plates were then incubated at 37 °C for 1 h. Samples were rinsed with PBS (without Mg^{2+} and Ca^{2+}) for 3 times followed by blocking with 500 µL of 5 wt% BSA solution (Sigma-Aldrich GmbH, Steinheim, Germany) at 37 °C for 2 h. After removing the blocking solution, 20 µL diluted HRP conjugated antibodies (all purchased from Abcam, Berlin, Germany) including anti-fibrinogen antibody (ab7539, 1:10,000, 2 wt% BSA), anti-albumin antibody (ab112989, 1:10,000, 2 wt% BSA) and anti-fibronectin antibody (ab25467, 1:5,000, 2 wt% BSA) were added and incubated with samples in dark and humid environment at room temperature for 1 h. Followed by 5 min washing, samples were then transferred to the new tissue culture plates. 300 µL TMB solution (Thermo Fischer Scientific, Nidderau, Germany) was added and incubated in dark at room temperature for 30 min. 70 µL supernatant from each sample was transferred into a 96-well plate and appropriate amount of stop solution (Thermo Fischer Scientific, Nidderau, Germany) was added into each well. Finally, the absorbance was measured using Infinite 200Pro microplate reader (Tecan, Wiesbaden, Germany) at a wavelength of 450 nm. Samples without platelet-poor plasma incubation were set as a control to substrate the background signal.

Bacterial culture

E. coli and MRSA purchased from LGC Standards GmbH (Wesel, Germany) were cultured in the BSL-2 lab of Berlin-Brandenburg Centre for Regenerative Therapies, Berlin, Germany. Bacteria were stored in cryovial bead preservation system (Microbank; PRO-LAB DIAGNOSTICS, Richmond Hill, ON, Canada) at 80 °C. Both bacteria were cultured on Columbia Blood Agar (VWR Chemicals, Leuven, Belgium) for 24 h at 37 °C in an ambient air incubator. Inocula were prepared according to a McFarland standard turbidity of 0.5 and determined by Colony Forming Units (CFUs) counting.

Microcalorimetry analysis of bacterial metabolism

For direct incubation, polymers were transferred to sterile calorimeter ampoules pre-filled with 4 ml MH broth containing MRSA or *E. coli* with the concentration of 5×10^5 CFUs/mL. For biofilm formation study, bacteria laden polymers were rinsed with PBS after bacterial adhesion for 24 h and transferred to the new ampoules with 4 ml pure 'Mueller Hinton broth (MH broth, Merck KGaA, Darmstadt, Germany). All test ampoules were closed with a rubber cap, sealed by manual crimping, and were sequentially introduced into the calorimetry instrument and remained for 15 min in the thermal equilibration position before being lowered into the measurement position. A 48-channel batch calorimeter (thermal activity monitor, model 3102 TAM III; TA Instruments, New Castle, DE, USA) was used to measure the heat flow at 37 °C controlled to within 0.0001 °C and had a sensitivity of 0.25 µW. Heat flow was measured at 10 s intervals during 24 h after the signal stability was achieved.

Fluorescent imaging of bacteria

For imaging of bacteria adhesion, MRSA or *E. coli* suspensions were incubated with material for 72 h. The imaging was based on glutaraldehyde induced fluorescence technique [6,22]. Polymers with bacteria were carefully removed, washed and treated with 1 wt% glutardialdehyde (Sigma-Aldrich GmbH, Steinheim, Germany) for one hour at room temperature. Subsequent to a thoroughly washing with PBS, material samples were embedded in Mowiol 4-88 mounting medium (Carl Roth GmbH, Karlsruhe, Germany). Images were captured using a confocal laser scanning microscope (LSM 510, Carl Zeiss, Jena, Germany).

Statistics

Data are presented as mean value ± standard deviation unless otherwise stated. At least three independent biological replicates were involved. GraphPad Prism was used for statistical

analysis (version 6.02, GraphPad Software Inc., San Diego, USA). Comparisons of the different groups were carried out by one-way analysis of variance (ANOVA). Bonferroni's multiple comparison tests were applied as post hoc analysis. p values of less than 0.05 were considered statistically significant.

Results and Discussion

Synthesis of mechanically and chemically stable polyGGE

Glycerol glycidyl ether (GGE), as a commercial available monomer in the epoxy resin family, is synthesized from glycerol and epichlorohydrin, involving two steps: formation of an intermediate chlorohydrin and dehydrohalogenation to form the glycidyl ether [23]. Polymerization of GGE took place though the typical steps for cationic ring-opening polymerization (**Fig. 1A**). Binding of epoxide onto the electrophilic cation formed by the photoinitiator followed by opening of the epoxide, forming an unstable carbocation that will be stabilized by the neighboring glycidyl ether, and chain propagation by iterative addition of monomer unit to the growing polymer chain. Theoretically, the resulting carbocation can continue to propagate until all epoxide rings open, which, however, is hindered by steric and mobility restrictions. The carbocation can be terminated by the presence of nucleophilic agents such as water. Due to the complexity of the monomer mixture, the monomer in **Fig. 1A** was illustrated as $C_3H_5O_2R$. This R-group might contain functional epoxy groups, which contributed to further crosslinks in the network.

As a thermosetting plastic, mechanical properties of polyGGE can be strongly influenced by many factors including post-curing temperature and UV exposure time [24]. In order to acquire favored properties of polyGGE, the tensile properties like Young's modulus (E) and elongation at break (ε_b) were investigated.

The Young's modulus of polyGGE within 60 min UV exposure ranged between 52 ± 12 MPa to 1440 ± 223 MPa, which increased drastically after every 10 min UV exposure. The elongation at break of polyGGE firstly increased from 2.5 ± 0.7 % to 12.2 ± 3.3 % and then decreased to 4.1 ± 1.3 %. The peak ductility of polyGGE film was reached by 30 min UV exposure (**Fig. 1B**). This could be demonstrated by the kinetics of the polyGGE network formation, which was mainly associated with forming a linear polyethylene glycol backbone and crosslinking between the chains. The growing length of segments in the backbone at the

initial stage of the polymerization enabled the increase of stretch ability of network. However, with the increasing number of epoxides in the side chains participating in chemical crosslinking, length of segments was decreased resulting in a low ductility of polyGGE.

To eliminate the unreacted epoxides and achieve a stable polymer network of polyGGE, the quenching approach was necessary to employed. It was known that base or water could be used to open the epoxide and terminate the propagation of the polymer chain [25,26]. In this context, 1 mol/L KOH aqueous solution was used. To determine the efficiency of quenching, ^{1}H NMR was used to analyze the residual epoxide inside the polyGGE network after KOD quenching at different time points (0, 4, 24 and 72 h). Resonance signals of protons of the methylene on oxirane ring at 2.80 and 2.60 ppm, and proton of methine on oxirane ring at 3.15 ppm were observed on the ^{1}H NMR spectra of unquenched polyGGE (0 h) and 4 h quenched polyGGE. When the quenching period was prolonged to 24 h reaching an equilibrium state of swollen (**Table 1**), no more resonance signals of protons on oxirane ring were traced, indicating a successful quenching of unreacted epoxides (**Fig. 1C**).

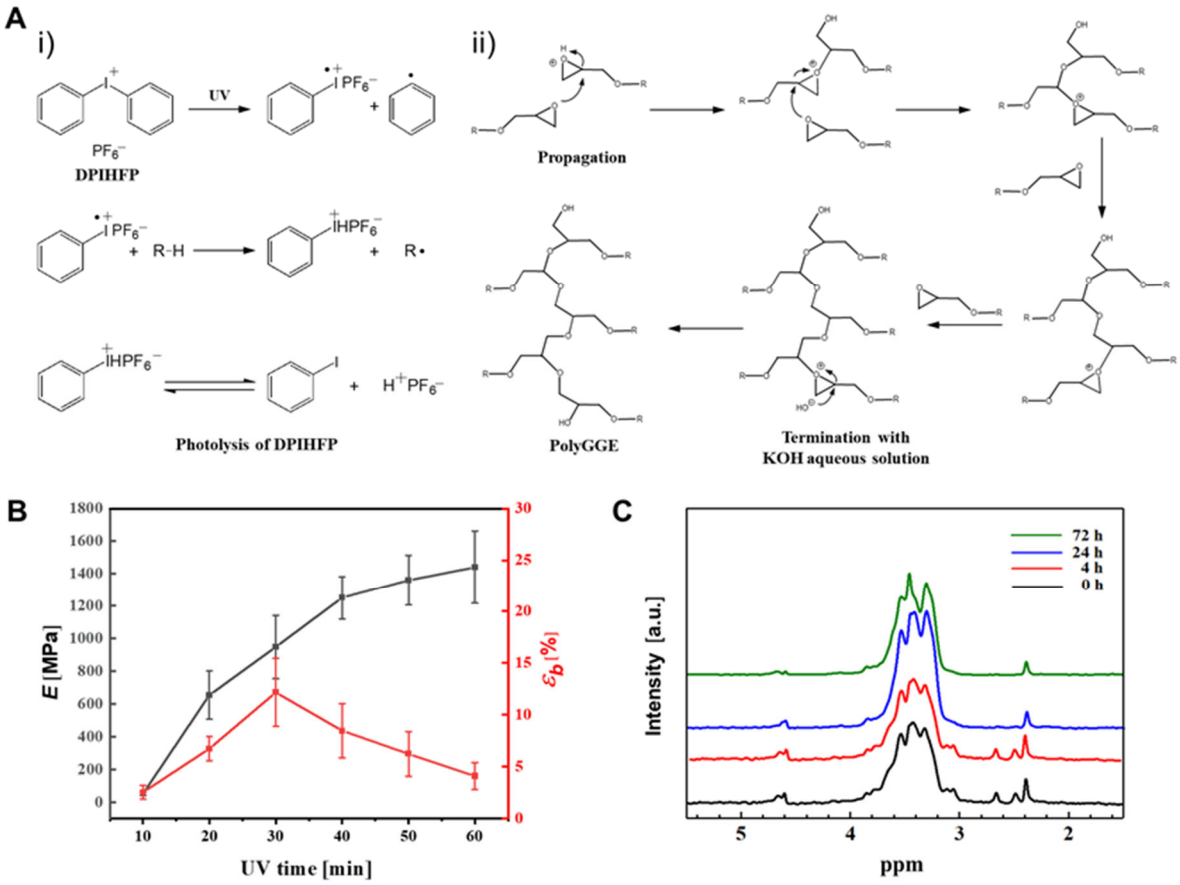

Fig. 1. Achieving mechanically and chemically stable polyGGE via adjusting UV curing and KOH quenching times. A. Schematic illustration of synthesis of bulk polyglycerol including **i)** photolysis of

the photoinitiator DPIHFP, **ii**) propagation and termination processes. **B.** Young's modulus (*E*, black) and elongation at break (ε_b, red) of 10, 20, 30, 40, 50 and 60 min UV-cured polyGGE films in dry condition at room temperature (n=3 independent experiments). **C.** ^{1}H NMR spectra of 30 min UV-cured polyGGE, which quenched by KOD for 0, 4, 24 and 72 h.

Mechanical and thermal properties of polyGGE at physiological conditions

The mechanical properties of polyGGE were determined at body temperature under aqueous conditions. In order to clarify whether heat drying after reaction termination at 24 h reactive time further influences the mechanical properties of polyGGE synthesized at various UV exposure times, samples with and without heat treatment were measured.

Neither the Young's modulus nor the elongation at break of heat-dried polyGGE differed from the non-heat-dried polyGGE (**Fig.2A-B**). While the Young's modulus of 30 min UV-cured polyGGE in wet state at body temperature was 37.5 ± 7.1 MPa, which is much lower than the value 948 ± 194 MPa measured in dry state at room temperature. PolyGGEs prepared with 10 and 20 min UV-curing exhibited similar Young's modulus (**Fig. 2A**). Decreased values of elongation at break were found for all swollen polyGGE materials, compared to dry samples. The highest ductility was found for polyGGE prepared by 30 min UV curing in hydrated condition at body temperature when compared to that in the dry state regardless of 24 h KOH quenching or additional one week 60 °C treatment (**Fig. 2B**).

These data indicate in the presence of water, polyGGE strongly changes its mechanical behavior. Approximately 6 wt% water were adsorbed into polyGGE prepared by 30 min UV curing and reached the equilibrium state after 24 h quenching in KOH aqueous solution (**Table 1**). Water might act as a softener and therefore swollen polyGGE are much softer yielding lower Young's modulus [15]. Previous studies revealed that water molecules in epoxy resins have very high affinity to the hydroxyl groups and the polyether backbone and can be classified in two types of bound water: (I) one water molecule forming one hydrogen bond with resin network, and (II) water molecules crosslinking in the network by multiple hydrogen bonds [27,28]. The diffusion of type I bound water into the polyGGE network breaks the initial inter-chain Van der Waals force resulting in an increase of chain segment mobility. The free volume in the network is replaced and expanded by water molecules, therefore, to a certain degree causing the reduced elongation at break. Moreover, the domination of type I bound water in the water sorption process aids to plasticize the polyGGE network and significantly reduce the Young's modulus of the polyGGE. Unlikely, Type II bound water molecules rather form

bridges between chain segments resulting in (pseudo crosslinking) secondary crosslinking than plasticization, which also contributes to the brittleness of the swelled polyGGE. It is also worth mentioning that, although type I bound water molecules can be removed by means of dryness, type II bound water molecules are relatively stable due to the higher activation energy and normally result in residual water or so-called locked-in water in the network, which interferes strongly the mechanical performance of the polymer.

Thermal stability of 30 min UV-cured, KOH quenched after 24 h, one week washed and one week 60 °C dried polyGGE, was monitored. TGA profiles showed that there was no major weight loss of polyGGE when heating up to 300 °C, beyond which a sharp weight loss is observed. During the continuous heating procedure, 1, 3 and 5.5% weight losses were found at 100, 200 and 300 °C, respectively (**Fig. 2C**). The minor weight loss before 200 °C might corresponding to the elimination of water molecule residuals. The weight loss between 200-300 °C could be associated with volatilization of polyGGE fragments with low polymerization degree [29]. The behavior of bulk degradation was similar to polyether glycol [30], which was assumed to occur with both -C-O- and -C-C- bonds of the backbone chain and started at around 340 °C and ended at 420 °C with a great weight loss of 82.8%. In the end, a residual weight of 7.6% remained (**Fig. 2C**). This result suggests that the polyGGE is thermal stable at body temperature and can be further heat sterilized.

PolyGGE is an amorphous polymer network with a glass transition temperature (T_g) at 33 °C in the dry state (**Fig. 2C**). One can expect that the mobility of polymer segmental chains will be enhanced and polyGGE can exhibit a softer and flexible state when warming up to body temperature (37 °C), which is higher than T_g.

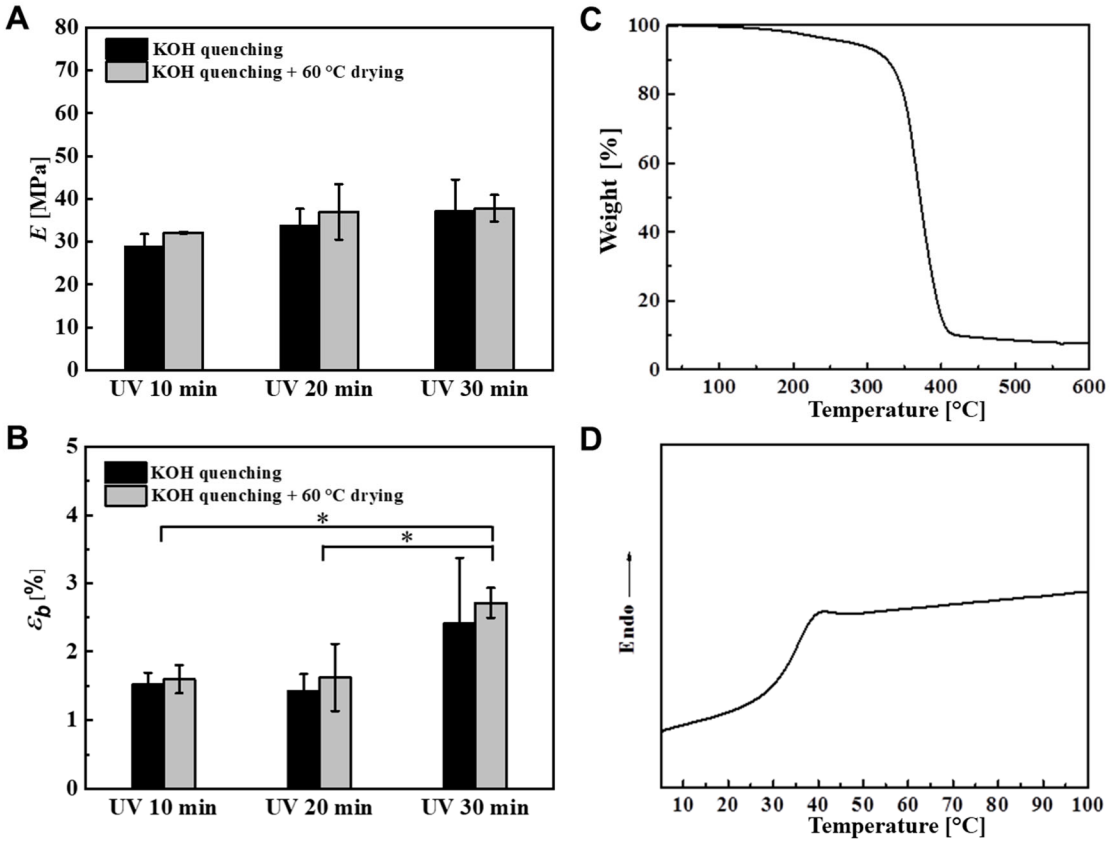

Fig. 2. PolyGGE with 30 min UV-curing and 24 h KOH quenching was mechanically and thermally stable at body temperature. Young's moduli (**A**) and elongation at break (**B**) of 10, 20 and 30 min UV-cured and 24 h KOH quenched polyGGE followed by one week washing and one week drying at 60 °C in wet condition at 37 °C (black, non-heat treated polyGGE; grey, heat-treated polyGGE. n≥3, *p<0.05, one-way ANOVA with Bonferroni's multiple comparison tests). TGA profile (**C**) and DSC heating curve (**D**) of 30 min UV-cured and 24 h KOH quenched polyGGE followed by one week washing and one week drying at 60 °C.

Table 1. Water uptake of polyGGE with different UV curing times

UV time (min)	1 h (wt%)	4 h (wt%)	20 h (wt%)	24 h (wt%)
10	3 ± 0.4	4 ± 0.5	9 ± 0.2	9 ± 0.3
20	1 ± 0.2	2 ± 0.3	6 ± 0.5	6 ± 0.5
30	1 ± 0.2	2 ± 0.3	6 ± 0.8	6 ± 0.7

Mean value ± standard deviation, n=3.

Resistance of plasma protein adsorption on PolyGGE surface

PolyGGE is considered to be a suitable polymer to resist protein adsorption due to the exhibition of its polyether backbone [31]. Thus, the adsorption of major human plasma proteins

including Fibrinogen, Albumin and Fibronectin was determined, which are highly involved in blood coagulation, wound healing, oncotic pressure regulation, and cell-receptor interaction with extracellular matrix [32-34]. Medical grade PDMS and PTFE were selected as control polymers in our investigation mainly due to their routine applications as medical devices and implants, which display high blood compatibility [35,36].

The adsorption of all plasma proteins on polyGGE and PDMS were significantly lower than that on PTFE. By comparing polyGGE to PDMS, it could be found that Fibrinogen adsorption on polyGGE was slightly higher than on PDMS while Albumin showed significantly lower adsorption on polyGGE rather than on PDMS. Fibronectin adsorption on polyGGE and PDMS did not differ (**Fig. 3A**). In general, the protein repelling ability of polyGGE is comparable with PDMS in spite of different mechanisms. Various physicochemical properties of polymer surfaces can affect the protein adsorption, such as hydrophilicity, charge, roughness and chemical structure [37]. Although the advancing water-air contact angle shows similar hydrophobicity nature for PDMS (advancing contact angle: 109 ± 3º) and PTFE (119 ± 3º) (**Fig. 3B**), these two polymeric materials showed different protein repelling ability (**Fig. 3A**). A hydrophobic surface exhibits high interfacial energy with water, which is the key to conferring the non-specific protein-resistant properties of the surface [38]. Amphiphilic biomolecules such as proteins show remarkable adsorption on the hydrophobic surface to minimize the interfacial energy, which can be seen on the surface of PTFE. However, non-polar surfaces of elastomeric polymers such as PDMS allow these adherent proteins to easily detach from the surface due to the low Young's modulus and surface energy. These have been widely explored as fouling release coatings. Hydrophilic surfaces like polyGGE (advancing contact angle: 71 ± 3º) (**Fig. 3B**), nevertheless, show a good resistance to plasma protein adsorption due to their sufficiently low polymer-water interfacial energy.

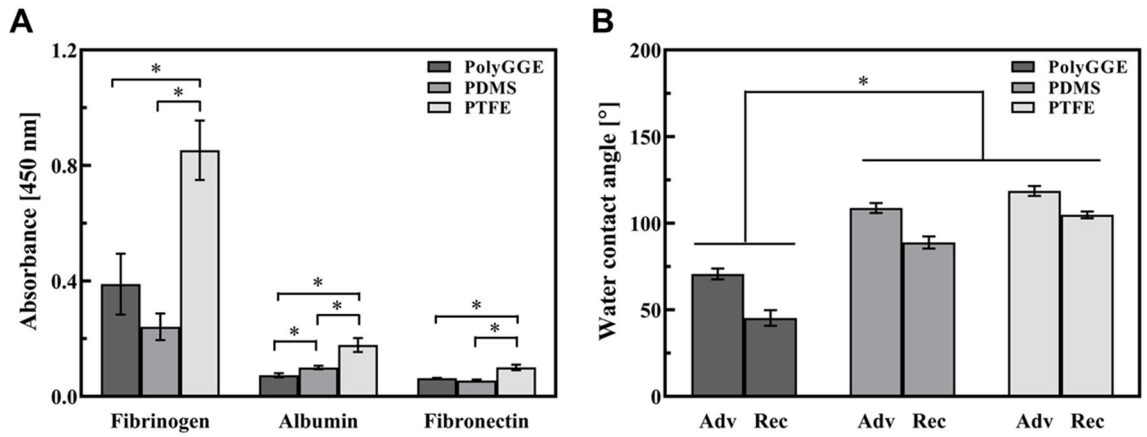

Fig. 3. Hydrophilic polyGGE surface resisted the adsorption of plasma proteins. A. Quantitative analysis of adsorption of Fibrinogen, Albumin and Fibronectin on polyGGE, PDMS and PTFE surfaces via ELISA (n=4, *p<0.05, one-way ANOVA with Bonferroni's multiple comparison tests for individual proteins). **B.** Water contact angle analysis as measured for the wettability of polyGGE, PDMS and PTFE surfaces (n=30, *p<0.05, one-way ANOVA with Bonferroni's multiple comparison tests).

Effect of polyGGE on antibiotic-resistant bacterial metabolism and biofilm formation

Micro-calorimetry is an innovative tool for quantitative assessment based on measuring heat from replicating microorganisms in culture [39]. The heat flows obtained from micro-calorimetry are proportional to the quantity of bacteria. The anti-bacterial fouling function of polyGGE was tested with both Gram- *E. coli* and Gram+ antibiotic-resistant *S. aureus* (MRSA) in direct contact.

The free-living planktonic bacteria with and without a porous glass bead (PC and PC beads) were set as positive controls due to their high sensitivity, reproducibility and simplicity. A negative control for each group (indicated as "-") constitutes by strip in fresh MH broth medium without any bacteria and the pure MH broth. Both bacteria showed fast growth within the initial 4h. The heat flow in PDMS and PTFE groups were comparable to the positive controls. Low heat flow of *E. coli* in the presence of polyGGE was then observed. The total heat of *E. coli* incubated with polyGGE was reduced by about 25% compared to positive controls (**Fig. 4A**). Similar results were observed for MRSA. The heat flow of MRSA in the presence of polyGGE was reduced apparently after 4 h and the total heat of MRSA was decreased by approximately 50% (**Fig. 4B**). These data suggest that the polyGGE can inhibit the metabolism not only for typical Gram- bacteria but also the Gram+ antibiotic-resistant bacteria with thicker and remolded cell wall [7,8].

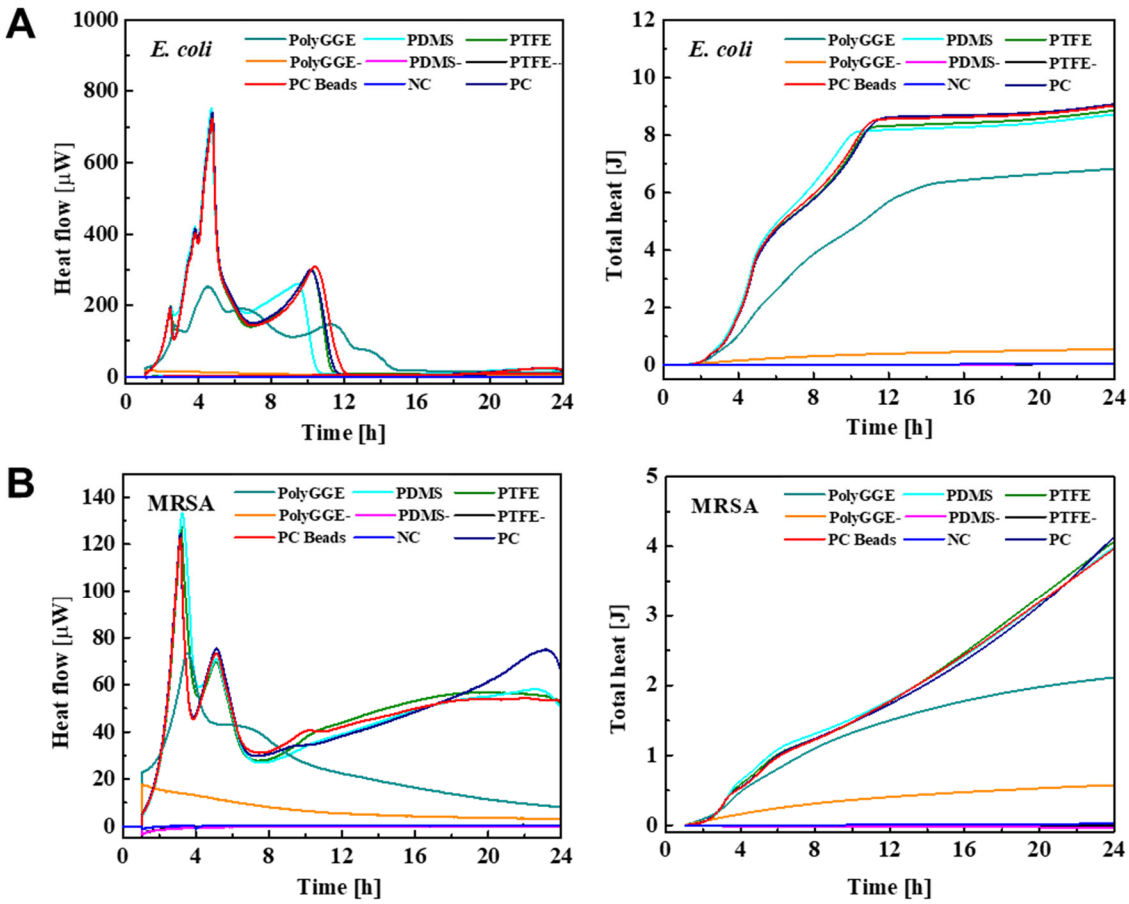

Fig. 4. PolyGGE interfered the metabolism conditions of *E. coli* and antibiotic-resistant MRSA. Thermokinetic profiles and the total heat derived from *E. coli* (**A**) and MRSA (**B**) with direct incubation of polyGGE, PDMS and PTFE. PC and PC beads were set as positive control. Bacteria-free material (polyGGE-, PDMS- and PTFE-) and pure MH broth medium (NC) were applied as negative controls.

Biofilm formations on polyGGE, PDMS and PTFE surfaces were monitored. According to the thermokinetics of heat generation of MRSA and *E. coli*, it was found that the polyGGE exhibited stronger influence on MRSA than *E. coli* (**Fig. 5A-B**). The total heat curve derived from MRSA biofilm on polyGGE was also depressed noticeably compared to that on PDMS (**Fig. 5B**). These results illustrated the underlying mechanism of the antifouling effect, which can be directed by polyGGE via interfering the status of bacterial metabolism especially for MRSA.

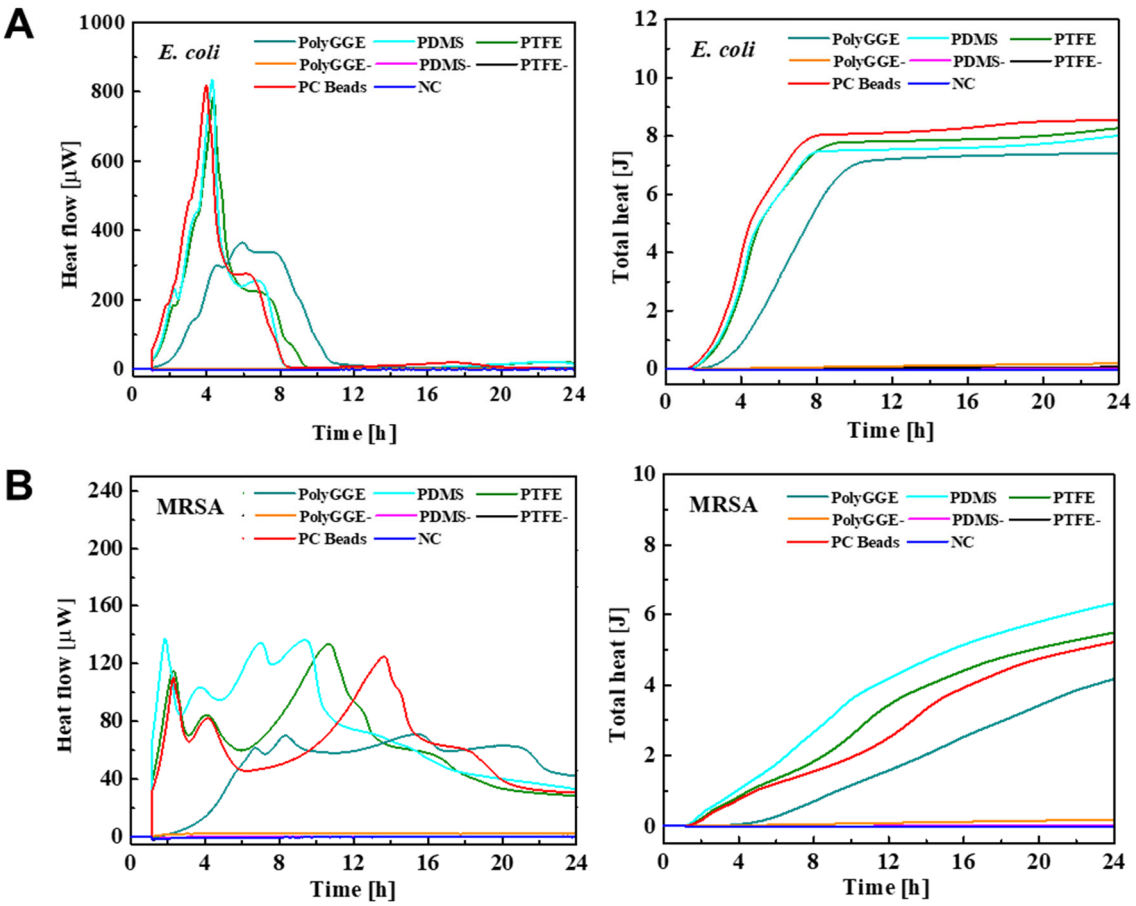

Fig. 5. PolyGGE retarded biofilm formation via metabolic inhibition of *E. coli* and antibiotic-resistant MRSA. Thermokinetic profiles and the total heat of biofilm formation from *E. coli* (**A**) and MRSA (**B**) attached (24 h post bacterial seeding) on polyGGE, PDMS and PTFE surfaces. PC beads was set as positive control. Bacteria-free material surfaces (polyGGE-, PDMS- and PTFE-) and pure MH broth medium (NC) were set as negative controls.

Bacterial biofouling and colonization were observed at the surfaces of PDMS and PTFE after 72 h culture, while only a few separate bacteria (both *E. coli* and MRSA) were found on polyGGE (**Fig. 6**). Among all three polymers, bacteria obtained after 72 h culturing time showed the greatest propagation on PDMS, which in consistent with micro-calorimetry data (**Fig. 5**). Although the elastomeric character of PDMS enabled itself to prevent plasma protein adsorption, PDMS was unlikely to prevent bacterial growth while polyGGE showed both anti-protein adsorption and anti-bacteria effect. In contrast to protein adsorption, bacteria-material interaction is much more complex. For hydrophobic materials like PDMS, the interfacial interactions can be stabilized to facilitate bacterial attachment in the presence of the hydrophobic cell wall composites, flagellum, pilli and the aligned hydrophobic functional groups on the material surface [4]. During the initial attachment, bacteria can experience short-range repulsive force in close proximity to negatively charged surfaces. The displacement of

water molecules near surfaces enhances hydrophobic interactions and promotes close contact between cells and surfaces [40]. Hydrophilic polyGGE can inhibit protein adsorption and repel bacterial adhesion. These properties are attributed to the steric repulsion of proteins and bacteria at interfaces where water molecules are coordinated to ether-based backbone of polyGGE and the rich hydroxyl end groups.

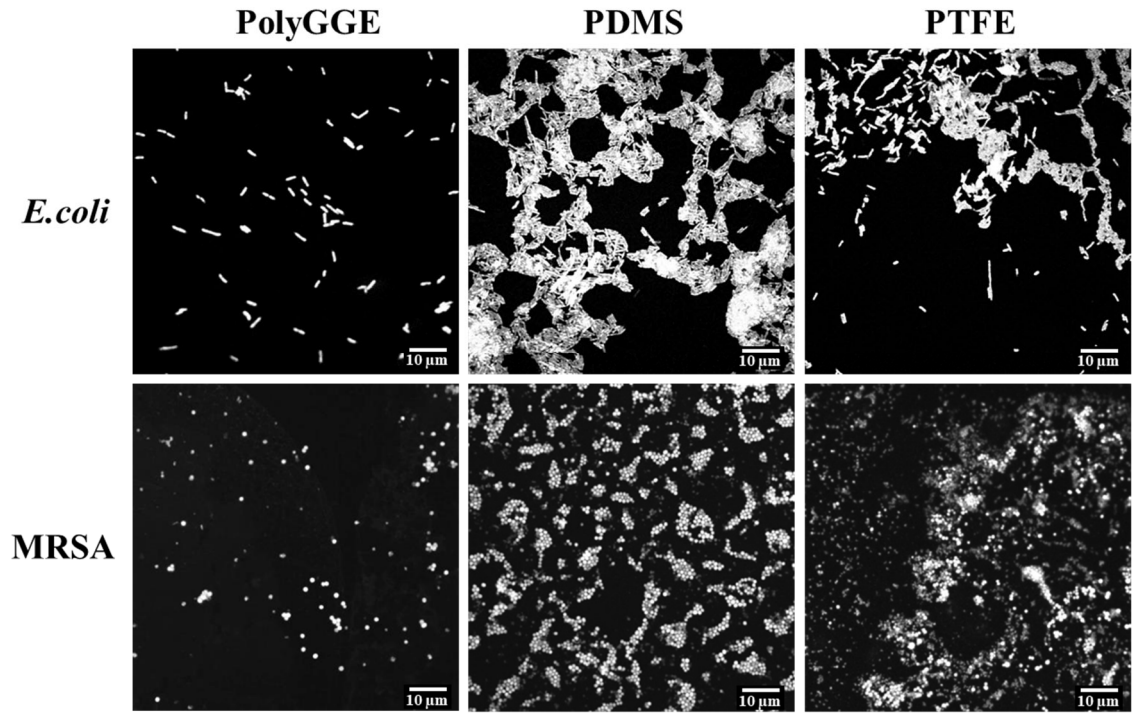

Fig. 6. PolyGGE inhibited growth and biofilm formation of *E. coli* (Gram- strain) and antibiotic-resistant MRSA (Gram+ strain). Representative confocal laser scanning microscopy images of bacteria (*E. coli* and MRSA) grown on polyGGE, PDMS and PTFE for 72 h. Scale bar = 10 μm.

Conclusions

PolyGGE was successfully polymerized from GGE monomer, which was characterized as a mixture of mono-, di- and tri-glycidyl ether. The cationic ring opening polymerization was carried out upon UV initiation of photoinitiator. Quenching with KOH aqueous solution for 24 h could efficiently eliminate the unreacted epoxides in the bulk. Although the Young's modulus in dry state could be altered by controlling the UV exposure time, only a minor difference between these samples was observed in wet state at 37 °C. The thermally stable polyGGE exhibits high ductility in case of 30 min UV-curing at physiological conditions. The hydrophilic polyGGE remarkably reduced the adsorption of Fibrinogen, Albumin and Fibronectin, which was comparable to the hemocompatible PDMS. PolyGGE could strongly inhibit the metabolism, biofilm formation and growth of both Gram- and Gram+ bacteria

including MRSA, the antibiotic-resistant *S. aureus*. The antifouling property of polyGGE highlighted its potential application for combating hospital-acquired infections. A potential application could arise from a combination of a starting material spray and UV curing, which could quickly form a transparent, permanent and scratch-resistant surface for daily used items in the hospital. Notably, the anti-MRSA effect of polyGGE also provides a possibility for its particular use in defeating the spread of deadly superbugs.

Acknowledgments

We thank Manuela Keller, Susanne Schwanz and Andrej Trampuz for technical support of water contact angle, DSC measurement, TGA analysis and bacterial maintenance. This work was financially supported by the Helmholtz Association of German Research Centers (through program-oriented funding, Helmholtz Cross Program Initiative "Technology and Medicine Adaptive Systems", Helmholtz Virtual Institute, Multifunctional Biomaterials for Medicine (Grant no. VH-VI-423)) as well as by the Federal Ministry of Education and Research, Germany through the Program Health Research (Grant no. 13GW0098).

References

[1] Damodaran VB and Murthy NS. Bio-inspired strategies for designing antifouling biomaterials. Biomater Res. 2016;20:18.

[2] Huang DN, Wang J, Ren KF and Ji J. Functionalized biomaterials to combat biofilms. Biomater Sci. 2020;8(15):4052-4066.

[3] Jamal M, Ahmad W, Andleeb S, Jalil F, Imran M, Nawaz MA, Hussain T, Ali M, Rafiq M and Kamil MA. Bacterial biofilm and associated infections. J Chin Med Assoc. 2018;81(1):7-11.

[4] Renner LD and Weibel DB. Physicochemical regulation of biofilm formation. MRS Bulletin. 2011;36(5):347-355.

[5] Tuson HH and Weibel DB. Bacteria-surface interactions. Soft Matter. 2013;9(18):4368-4380.

[6] Costa OYA, Raaijmakers JM and Kuramae EE. Microbial Extracellular Polymeric Substances: Ecological Function and Impact on Soil Aggregation. Front Microbiol. 2018;9:1636.

[7] Mai-Prochnow A, Clauson M, Hong J and Murphy AB. Gram positive and Gram negative bacteria differ in their sensitivity to cold plasma. Sci Rep. 2016;6:38610.

[8] Lee AS, de Lencastre H, Garau J, Kluytmans J, Malhotra-Kumar S, Peschel A and Harbarth S. Methicillin-resistant Staphylococcus aureus. Nat Rev Dis Primers. 2018;4:18033.

[9] Hu X, Kang F, Yang B, Zhang W, Qin C and Gao Y. Extracellular Polymeric Substances Acting as a Permeable Barrier Hinder the Lateral Transfer of Antibiotic Resistance Genes. Front Microbiol. 2019;10:736.

[10] Schottler S, Becker G, Winzen S, Steinbach T, Mohr K, Landfester K, Mailander V and Wurm FR. Protein adsorption is required for stealth effect of poly(ethylene glycol)- and poly(phosphoester)-coated nanocarriers. Nat Nanotechnol. 2016;11(4):372-7.

[11] Busscher HJ, Ploeg RJ and van der Mei HC. SnapShot: Biofilms and biomaterials; mechanisms of medical device related infections. Biomaterials. 2009;30(25):4247-8.

[12] Turecek PL, Bossard MJ, Schoetens F and Ivens IA. PEGylation of Biopharmaceuticals: A Review of Chemistry and Nonclinical Safety Information of Approved Drugs. J Pharm Sci. 2016;105(2):460-475.
[13] Garay RP, El-Gewely R, Armstrong JK, Garratty G and Richette P. Antibodies against polyethylene glycol in healthy subjects and in patients treated with PEG-conjugated agents. Expert Opin Drug Deliv. 2012;9(11):1319-23.
[14] Sellaturay P, Nasser S, Islam S, Gurugama P and Ewan PW. Polyethylene glycol (PEG) is a cause of anaphylaxis to the Pfizer/BioNTech mRNA COVID-19 vaccine. Clin Exp Allergy. 2021;51(6):861-863.
[15] Ekinci D, Sisson AL and Lendlein A. Polyglycerol-based polymer network films for potential biomedical applications. J Mater Chem. 2012;22(39):21100-21109.
[16] Dektar JL and Hacker NP. Photochemistry of diaryliodonium salts. J Org Chem. 1990;55(2):639-647.
[17] Cattaneo M, Cerletti C, Harrison P, Hayward CP, Kenny D, Nugent D, Nurden P, Rao AK, Schmaier AH, Watson SP, Lussana F, Pugliano MT and Michelson AD. Recommendations for the Standardization of Light Transmission Aggregometry: A Consensus of the Working Party from the Platelet Physiology Subcommittee of SSC/ISTH. J Thromb Haemost. 2013.
[18] Harrison P, Mackie I, Mumford A, Briggs C, Liesner R, Winter M, Machin S and British Committee for Standards in H. Guidelines for the laboratory investigation of heritable disorders of platelet function. Br J Haematol. 2011;155(1):30-44.
[19] Berg B, Solberg HE, Nilsson JE and Tryding N, Practical experience in the selection and preparation of reference individuals: Empirical testing of the provisional Scandinavian recommendations. in: Gräsbeck R, Solberg HE, and Alström T, (Eds.). Reference Values in Laboratory Medicine: The Current State of the Art, Wiley, Michigan, 1981;55-64.
[20] Braune S, Latour RA, Reinthaler M, Landmesser U, Lendlein A and Jung F. In Vitro Thrombogenicity Testing of Biomaterials. Adv Healthc Mater. 2019;8(21):e1900527.
[21] Braune S, Walter M, Schulze F, Lendlein A and Jung F. Changes in platelet morphology and function during 24 hours of storage. Clin Hemorheol Microcirc. 2014;58(1):159-70.
[22] Ethical guidelines for publication in Clinical Hemorheology and Microcirculation. Clin Hemorheol Microcirc. 2010;44(1):1-2.
[23] Crivello JV. Design and synthesis of multifunctional glycidyl ethers that undergo frontal polymerization. J Polym Sci Part A: Polym Chem. 2006;44(21):6435-6448.
[24] Park Y-J, Lim D-H, Kim H-J, Park D-S and Sung I-K. UV- and thermal-curing behaviors of dual-curable adhesives based on epoxy acrylate oligomers. International Journal of Adhesion and Adhesives. 2009;29(7):710-717.
[25] Nuyken O and Pask SD. Ring-Opening Polymerization—An Introductory Review. Polymers. 2013;5(2).
[26] Hansen T, Vermeeren P, Haim A, Dorp M, Codée J, Bickelhaupt FM and Hamlin T. Regioselectivity of Epoxide Ring‐Openings via SN2 Reactions Under Basic and Acidic Conditions. Eur J Org Chem. 2020;2020:3822-3828.
[27] Mani S, Khabaz F, Godbole RV, Hedden RC and Khare R. Structure and Hydrogen Bonding of Water in Polyacrylate Gels: Effects of Polymer Hydrophilicity and Water Concentration. J Phys Chem B. 2015;119(49):15381-93.
[28] Zhou J and Lucas JP. Hygrothermal effects of epoxy resin. Part I: the nature of water in epoxy. Polymer. 1999;40(20):5505-5512.
[29] Díaz-Lasprilla AM, Mercado RA and Ramírez-Caballero GE. Glycerol polymerization degree effect on the emulsifying properties of polyglycerol esters. J Appl Polym Sci. 2021;138(24):50566.
[30] Jiang G, Ponnapati R, Pernites R, Felipe MJ and Advincula R. Surface-Initiated Ring-Opening Metathesis Polymerization (SI-ROMP): Synthesis and Electropolymerization of Terthiophene-Functionalized Olefin Peripheral Dendrons. Macromolecules. 2010;43(24):10262-10274.

[31] Lowe S, O'Brien-Simpson NM and Connal LA. Antibiofouling polymer interfaces: poly(ethylene glycol) and other promising candidates. Polym Chem. 2015;6(2):198-212.
[32] Zuliani-Alvarez L and Midwood KS. Fibrinogen-Related Proteins in Tissue Repair: How a Unique Domain with a Common Structure Controls Diverse Aspects of Wound Healing. Adv Wound Care. 2015;4(5):273-285.
[33] Maitra S and Dutta D, Chapter 18 - Salt-induced inappropriate augmentation of renin–angiotensin–aldosterone system in chronic kidney disease. in: Preuss HG, and Bagchi D, (Eds.). Dietary Sugar, Salt and Fat in Human Health, Academic Press, 2020;377-393.
[34] Parisi L, Toffoli A, Ghezzi B, Mozzoni B, Lumetti S and Macaluso GM. A glance on the role of fibronectin in controlling cell response at biomaterial interface. Jpn Dent Sci Rev. 2020;56(1):50-55.
[35] Jung YG, Kim HY, Dhong HJ, Park KN, Lee HJ, Lim YJ and Min JY. Ultrasonographic monitoring of implant thickness after augmentation rhinoplasty with expanded polytetrafluoroethylene. Am J Rhinol Allergy. 2009;23(1):105-10.
[36] Streller U, Sperling C, Hubner J, Hanke R and Werner C. Design and evaluation of novel blood incubation systems for in vitro hemocompatibility assessment of planar solid surfaces. J Biomed Mater Res B Appl Biomater. 2003;66(1):379-90.
[37] Rana D and Matsuura T. Surface Modifications for Antifouling Membranes. Chem Rev. 2010;110(4):2448-2471.
[38] Krishnan S, Weinman CJ and Ober CK. Advances in polymers for anti-biofouling surfaces. J Mater Chem. 2008;18(29):3405-3413.
[39] Thein E, Tafin U, Betrisey B, Trampuz A and Borens O. In Vitro Activity of Gentamicin-Loaded Bioabsorbable Beads against Different Microorganisms. Materials. 2013;6(8):3284-3293.
[40] Berne C, Ellison CK, Ducret A and Brun YV. Bacterial adhesion at the single-cell level. Nat Rev Microbiol. 2018;16(10):616-627.